

Methods of Analysis of Organic Light Emitting Diodes[†]

DANIEL DE SÁ PEREIRA^{1*}, PRZEMYSŁAW DATA^{1,2,3} AND ANDREW P. MONKMAN¹

¹Physics Department, Durham University, South Road, Durham DH1 3LE, United Kingdom

²Faculty of Chemistry, Silesian University of Technology, M. Strzody 9, 44-100 Gliwice, Poland

³Center of Polymer and Carbon Materials, Polish Academy of Science, M. Curie-Skłodowskiej 34, 41-819 Zabrze, Poland.

Received: September 20, 2016. Accepted: October 27, 2016.

Having revolutionized the smartphone and flat panel displays industry, Organic Light Emitting Diodes (OLEDs) have already become a multibillion dollar industry with more and more famous companies investing in this technology for their applications. Research in this area is growing at a fast rate resulting in different areas such as chemistry, physics and engineering to work together in order to improve the devices' efficiencies, power saving and overall simplicity. In this review, the basic mechanism inside an OLED is analysed and the basic characterization (electrical and optical) overviewed.

Keywords: Organic Electronics, OLEDs, Charge Carriers, Recombination, External Quantum Efficiency.

1. INTRODUCTION

Due to the unique electrical (and optical) properties of organic semiconductors which is a result of the nature of carbon's atomic orbitals and the bonds that these carbon atoms form with other atoms, Tang and Vanslyke were the first to report the emission of light from organic electroluminescence devices [1]. With the resulting extensive research in the area, Organic Light Emitting

Corresponding author e-mail: daniel.a.pereira@durham.ac.uk

[†]The research leading to these results received funding from the H2020-MSCA-ITN-2015/674990 project "EXCILIGHT".

Diodes (OLEDs) have been recently applied in a large number of today's state-of-the-art mobile phone and Flat Panel Displays (FPD) and are now starting to change the Solid State Lighting (SSL) industry as well [2], [3]. Other applications include head-mounted micro displays for augmented-reality applications while organic sensors for biomedical applications comes as a more futuristic application, given the need for high luminance and stability [4]. An OLED is composed with a set of organic layers, each with a specific function in the overall device, sandwiched between two electrodes. Their operation (**Figure 1**) is based on the injection of opposite carriers (electrons and holes, **Figure 1a**) from different sides of the electrodes to the organic layers, where they hop through the molecular structure of each individual compound (**Figure 1b**). These then meet in a specific layer (**Figure 1c**) to promote exciton recombination (**Figure 1d**) – the electron relaxes to the hole resulting in the emission of a photon with a wavelength corresponding to this relaxation, this being a characteristic of the layer where the recombination occurs [5]. With this mechanism in mind, it is possible to design structures that promote carrier injection, transport, or blockage in order to have recombination in specific layers and achieve the highest efficiency at the lowest power consumption, always having in mind their energy levels, particularly the Highest Occupied Molecular Orbitals (HOMO) and Lowest Unoccupied Molecular Orbitals (LUMO). Careful design strategies can be applied which will have significant effects in device aspects such as emission wavelength, lifetime, stability, efficiency and heat generation. Moreover, the design of

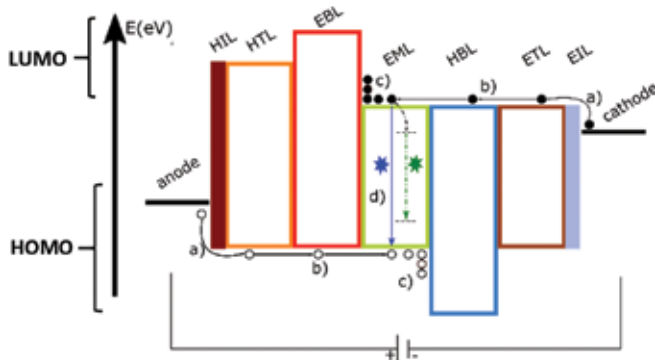


FIGURE 1

OLED structure according to the HOMO and LUMO energy levels of each layer and physical mechanism describing all individual steps: a) carrier injection, b) carrier transport, c) carrier blockage, d) exciton recombination. Different layers are denoted according to 1) the charge it relates to (hole or electron) and 2) its basic function (injection, transport or blockage) giving rise to the Hole and Electron Injection (HIL and EIL respectively), Transport (HTL and ETL respectively) and Blocking (HBL and EBL respectively) layers. Finally, recombination and emission takes place in the Emissive Layer (EML) either via fluorescence (straight blue line) or phosphorescence (dashed green line) [5].

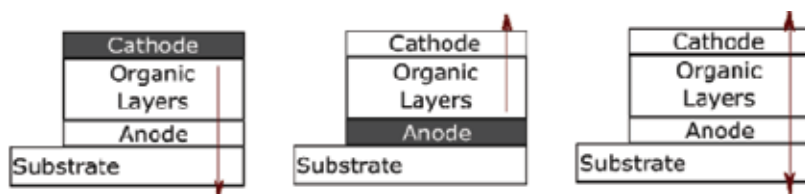


FIGURE 2
Different types of OLEDs. From left to right, the bottom emitting, top emitting and transparent OLEDs, are shown, respectively.

certain molecules with particular parameters plays an important role as they can be synthesised to have specific emissions and finally tune the overall device performance [6], [7].

An OLED can be classified accordingly to the architecture applied. The bottom emitting has the photons being extracted from a transparent anode (with low roughness and high work function such as Indium Tin Oxide – ITO) situated on top of a substrate (either plastic, glass, or metal foil, which is a transparent and conductive substrate with high work function) with a metallic cathode, the most common being Aluminium. Light extraction from the top electrode device with the use of a transparent cathode (with transparent low work function metal alloys such as Mg:Ag) while a fully transparent device can also be produced though the design structure involved are more complex [8]. All structures are shown in **Figure 2**.

2. CHARACTERIZATION OF OLEDS

In order to evaluate the total brightness output and performance characteristics of an OLED and its applicability into more complex applications, a set of characterizations, both electrical and optical, is required. This gives comprehension on parameters such as power consumption, efficiency, colour figures of merit, among others, achieved with a specialized equipment prepared to run all the necessary equations given the information that is provided compared to the one obtained.

2.1. Electrical

The characterization of a light system is based on a set of empirical standardized definitions for each individual system allowing possible comparison to others. It is then important to have these definitions when researching possible new light systems. First, the luminous flux (given in lumen, lm) is defined as amount of light capable of sensitizing the human eye per unit of time, or the total photometric power emitted in all directions from a light source. It is standardized with the (ideal) eye's maximum sensitivity, at 555 nm (or 1/680 W). The luminous intensity (measured in candela, cd) takes into account the colour of the light and its direction. It is the luminous flux

TABLE 1
Photometric Quantities [9].

Quantity	Definition	Units
Luminous flux	Radiant flux capable of producing visual sensation	Lumen (lm)
Luminous Intensity	Luminous flux emitted in a narrow cone that contains the given direction divided by the solid angle of the cone	Candela (cd) Lumen/meter ² (lm/m ²)
Illuminance	Luminous flux per unit of area at a point on a given surface	Candela/meter ² (cd/m ²)
Luminance	Luminous Intensity per unit of area at a point of a given surface	(cd/m ²)

emitted in to a specific solid angle. Finally, the Illuminance, I , and the Luminance, L , are the luminous flux and luminous intensity, both per unit of area, respectively [9].

In application, typical brightness levels of mobile displays are between 100-400 cd/m^2 while for general illuminations, higher values of around 5000 cd/m^2 are required.

The current efficiency can be calculated as the amount of current flowing through the device, J , with an emissive area, S , necessary to produce a certain Luminance, L , expressed by the equation 1 in cd/A .

$$\eta_L = \frac{L}{J} = \frac{LS}{I} \quad (1)$$

The luminous efficacy, as another means to characterize the device's performance, given by the ratio of the optical flux to the electrical input. Considering the current efficiency at an applied voltage, V_i it is given by equation 2 in unit of lm/W .

$$\eta_p = \eta_L \frac{f_D \pi}{V_i} \quad (2)$$

Where f_D (equation 3) is the angular distribution of the emitted light in the forward hemisphere considering its two angles and the light intensity measured in the forward direction.

$$f_D = \frac{1}{\pi I_0} \int_0^{\pi/2} \int_{-\pi}^{+\pi} I(\theta, \varphi) \sin(\theta) d\varphi d\theta \quad (3)$$

The External Quantum Efficiency, E.Q.E. (η_{ext}) is given by the ratio between the number of photons emitted from the surface of the device and the number of injected electrons. It can also be expressed by the product between the Internal Quantum Efficiency, I.Q.E. (η_{int}) and the outcoupling efficiency (η_{out}) – equation 4.

$$\eta_{ext} = \eta_{int} \cdot \eta_{out} \quad (4)$$

While η_{int} depends on the device architecture and the quantum yield of the charge recombination process, η_{out} is more dependent on the direction and propagation via external modes i.e. the actual light that escapes from the substrate surface, opposed to the internal modes which remain trapped inside the device substrate and waveguide modes as shown in Figure 3.

The key in optimizing the two parameters from equation 4 is to achieve an efficiency close to unity. The I.Q.E., for example, can be rewritten – equation 5 – as the product between the charge balance factor, γ or the fraction of injected carriers that form excitons, the fraction of spin-allowed excitons, η_{ST} and the Photoluminescence Quantum Yield (PLQY, or Φ_{PL}) which is a property of the molecule [5].

$$\eta_{int} = \gamma \cdot \eta_{ST} \cdot \Phi_{PL} \quad (5)$$

In a well-optimized device with perfectly matched electron and hole currents, Φ_{PL} could also reach near unity, the can also be close to one, depending on emitter molecular optimization. However, η_{ST} can vary depending on the type of emitter used in the device, fluorescent or phosphorescent, which is ruled by the 1:3 ratio of singlet to triplet exciton ratio formed on charge recombination and governed by quantum spin statistics [10].

Different emitter classes have limited achievable maximum IQE's; fluorescent, phosphorescent, Thermally Activated Delayed Fluorescent (TADF) or enhanced fluorescent. A fluorescent emitter can only emit from singlet excitons, limiting η_{ST} to 25% (**Figure 4a**), phosphorescent emitters can emit from both singlet and triplet excitations – as phosphorescence at the triplet excitation energy (**Figure 4b**) – whereas TADF emitters can convert triplet excitations to singlet states and emit at the singlet energy, so that both types can reach η_{ST} to 100%. This can be achieved by using heavy metal atoms with strong Spin-Orbit coupling to promote Intersystem Crossing (ISC) and triplet emission for the phosphorescent emitter. Specific molecular design with a small singlet triplet energy gap (<0.2 eV) enables Reverse ISC (RISC) via thermal activation in TADF emitters. The recent use of TADF systems shows great potential in avoiding the use of expensive and often instable metal phosphors but they still suffer from problems such as lower brightness and lifetimes when com-

pared to these typical phosphor based devices. The enhanced fluorescent mechanism (**Figure 4d**) involves the use of a blend with a TADF molecule and a typical fluorescent emitter. Here, the first transfers energy to the second (more information on energy transfer mechanisms can be seen in [5], [11]), overcoming the 25% limitation imposed for the fluorescent emitter. More information on all these four systems can be found elsewhere [5], [12], [13].

Considering out-coupling, the idea is to develop structures that could decrease light trapping inside the bulk of the device (**Figure 3**). While 50 to 60% of the total light produced remains confined in the device due to variation in refractive index of the different materials making the device (total internal reflection) and various internal loss mechanisms. approximately 20 to 30% is wasted in the form of Total Internal Reflection given the difference in the refractive index at the glass-air interface (substrate modes). By optimizing the light extraction efficiency, the overall E.Q.E. of the devices can be greatly improved so, strategies have successfully applied, reviewed elsewhere [5], [11], which mainly include refractive index matching or nano-sized features to decrease the plasmonic losses in the metallic cathode, light effectively absorbed by the cathode metal. E.Q.E.s up to 63% have been reported for a phosphorescent green OLED when employing these techniques [14]. Finally, the use of horizontally oriented molecular dipoles upon evaporation may also improve the out-coupling of light, this being responsible for E.Q.E.s of, for example, 37% in TADF based OLED [13].

2.2. Optical

For illumination purposes, a light source's quality is characterized accordingly to empirical figures of merit correspondent to each source that enables to qualitatively define the colour quality of such devices. It is possible to address these for different colour sources and see how optically efficient they are for the application in mind. These criteria have been sent down as standards by the Commission Internationale d'Eclairage (CIE) chromaticity coordinates (x,y) and also include the Correlated Colour Temperature (CCT) and the Colour Rendering Index (CRI).

3. CIE 1931 (x, y)

The human eye perceives light intensity and colour as a result of a cerebral interpretation from the behaviour of two different types of cells in the human eye's retina: the rod and the cone cells, respectively. The rod cells are more sensitive than cones, easily saturating under high ambient illumination. The cone cells, on the other hand, function well under brighter conditions giving

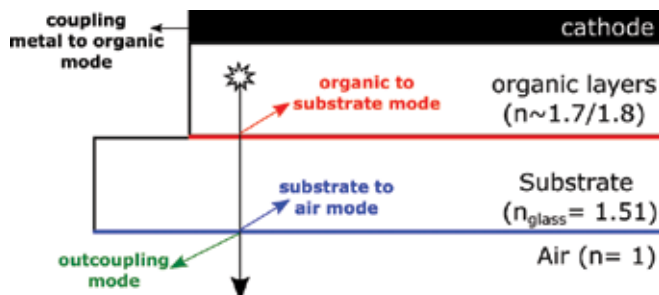


FIGURE 3
Light modes inside an OLED

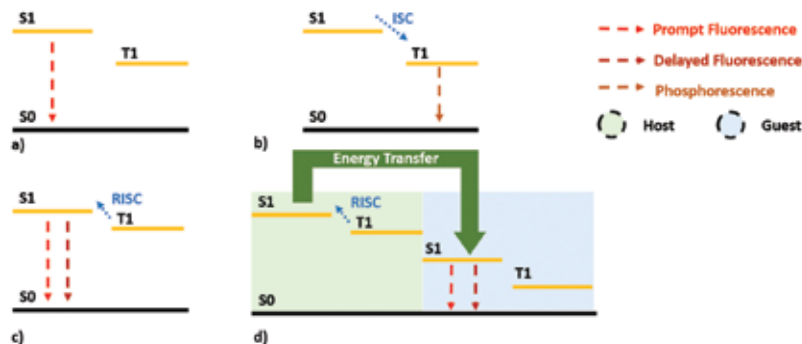


FIGURE 4
Mechanisms responsible for the emission of light with regard to the spin statistics: a) fluorescence, b) phosphorescence, c) Thermally Activated Delayed Fluorescence (TADF), d) Enhanced Fluorescence. TADF is commonly seen in Inter or Intramolecular Charge Transfer (CT) complexes if the CT state is formed either inside one Donor-Acceptor (DA) – inter – entity or between two separate – intra – D and A moieties.

rise to colour sensitivity, being composed of three independent retinal compounds, stimuli sensitive to three main groups of wavelengths – Red, Green and Blue (RGB) with large overlap. In combination, while one controls the eye response to different illuminate sources, the other reacts to the different colours emitted. Therefore, all colours can be expressed as a combination of the three primary colours. Every colour in the visible range was adapted into a three coordinates space – X, Y and Z respectively – and so the CIE 1931 (X, Y, Z) was created. Following various linear transformations of these tristimulus RGB, the CIE 1931 (x, y) was adapted, a horseshoe-shaped diagram where each boundary represents a monochromatic light. A diagram like this can now serve as an optical comparison of all different sources, either lab produced or industry available [15].

4. CCT

True ‘colour temperature’ is the colour of radiation emitted from a perfect blackbody radiator held at a particular temperature, being defined in units of Kelvin. The light of an incandescent bulb which comes from thermal radiation approximating closely a black body, so that the colour temperature associated with the temperature of the filament and the light spectrum emitted are well defined. Light sources other than incandescent lamps are described in terms of the Correlated Colour Temperature, CCT. The CCT is the temperature of a blackbody radiator that has a colour that most closely matches the emission from the non-blackbody radiator which can also be obtained with the EL spectrum. **Figure 5** shows the CIE 1931 used for optical characterization including different colours regions and temperatures. The arc represents the Planckian locus, the coordinates of black body radiation at temperatures ranging from 1500 to 10000 K. A pure white source has chromaticity coordinates close to the Equal Energy White (0.33, 0.33) [16]. **Figure 6** contains different sources and corresponding CCT.

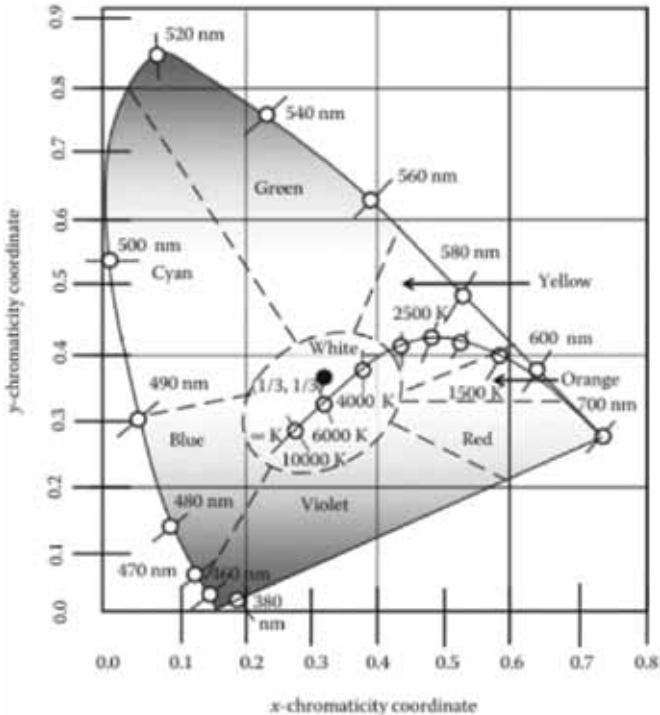


FIGURE 5

CIE 1931 (x,y) including different colour regions, planking locus and colour temperatures [16]

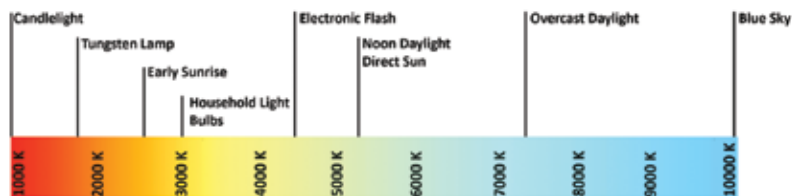


FIGURE 6
Different light sources and corresponding colour temperatures.

5. CRI

The Colour Rendering Index (CRI) is the measure of how well a light source can reproduce its environment colours, quantifying how different a set of test colours appear when illuminated by the source compared to when the same test colours are illuminated by the standard illuminate with the same correlated colour temperature. The CRI is obtained from a set of calculations having the Electroluminescence spectrum of a certain OLED source adapting it to a 0-100 scales, with 100 representing true colour perfection. A monochromatic light, such as an orange lamp will only ever render orange colours resulting in a poor CRI whereas a polychromatic light with balanced RGB counterparts will be able to reproduce all different colours from different objects and thus, a high CRI will be seen. So, depending on the application (such as general lighting), it is important that light sources possess good colour rendering as to ensure that objects appear as natural as they really are. CRI is often used to define the quality of a light source.

The calculation of the Colour Rendering is based on the comparison of a given light source with a set of reference coloured cards, this depending of the colour temperature of the source in study – for colour temperatures above 5000 K the reference should be the CIE daylight coordinates while lower temperatures should use of the blackbody radiator as a reference. Alternatively a method for calculating the colour rendering uses a set of illuminants having the same or nearly the same colours (chromaticities) as the test sources, but with precisely defined spectral power distributions, such as those for standard daylights for bluish sources and those for Planckian radiators for yellowish sources. Hunt and Pointer describe the method for both these calculations in their book, “Measuring Colour” [17].

As an example of the differences in the lighting figures of merit, **Figures 7 and 8** show two different studies, one for the colour tuning abilities of a RGB blend shown in terms of CCT and CIE with a high CRI for a system [18] while the other shows the figures of merit of a monochromatic emission and its main effect in the CRI [19].

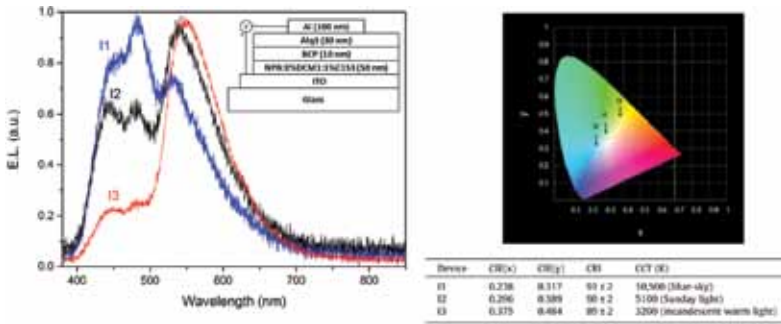


FIGURE 7 Study of a device structure with a colour tuning effect in a White OLED, this being in terms of its figures of merit. Given the broad EL spectra of the different devices, hence covering the entire electromagnetic spectrum, the CRI showed a high value. The device structure is shown in the inset of the EL spectra while the figures of merit are shown in the table and CIE diagram [18].

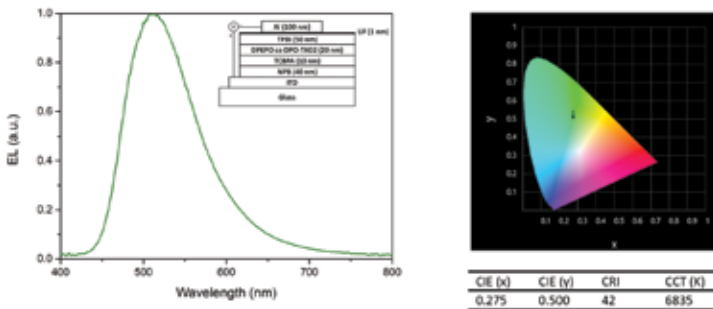


FIGURE 8 Study of the application of a TADF molecule for a high efficient device with a monochromatic emission. The corresponding figures of merit prove its monochromatic behaviour and the CRI was, as expected, low. The device structure is shown in the inset of the EL spectra while the figures of merit are shown in the table and CIE diagram [19].

5.1. Integrating sphere

The optoelectrical performance of OLEDs and other SSL sources can be measured with an integrating sphere, the diameter of sphere being dictated by the size of the device under test, having the standard guidelines on how photometric, radiometric, and colorimetric quantities for individual OLEDs should be measured in labs. An integrating sphere collects all the light from a source placed inside it, i.e. into 4π radians solid angle. More specifically, given a lambertian emitter (the brightness of a lambertian source is independent of the viewing angle) of a typical OLED, the measurement device must capture light from all directions so, the configuration must allow an integration over 4π steradian of solid angle (i.e. an entire sphere). The set-up con-

sists of a holder inside of the sphere connected to a source meter that will give the current-voltage curve of each device. Also, coupled with the source meter, a calibrated photodiode and a spectrometer give information on the luminous intensity and Electroluminescent (EL) spectrum of the source, respectively, with the light being totally reflected inside the sphere. The sphere is thus coated on the inside with a high reflective material with a minimal spectral dependence over a large spectral range, larger the source being measured.. Finally, with the emitting area, a computer software does all the calculations necessary for the characterization of the source, producing all the typical plots characteristic of the devices: Voltage-Current Density-Luminance (JVL), Current density-E.Q.E.- luminous efficacy, Luminance-current efficiency-E.Q.E. from the opto-electrical data and all the figures of merit (CIE, CCT and CRI) extrapolated from the EL. This will shine lights on different aspects such as maximum brightness, efficiency roll-off, device lifetime, among others.

5.2. Setting up an integrating sphere

When using an integrating sphere in the lab, a NIST calibration lamp must be used to determine the correct and standardized device efficiency by taking account of the response of the measurement system as a whole. The calibration lamp (with a known (certified) power spectrum output, $P_{cal}(\lambda)$ in W/nm) is positioned with the same experimental setup (sample position) used for the devices (which will have a power spectrum output, $P_{dev}(\lambda)$ in W/nm) . By applying a constant current, the intensity of the lamp, $I_{cal}(\lambda)$ is measured and the Reference spectra, $R(\lambda)$ calculated from equation 6. The shape and size of calibration lamp also effects the measurement, so an 'Auxiliary' spectra is also measured, which elicits the optical interference of the device holder and standard lamp on the response of the sphere. An Auxiliary lamp (having known power spectrum referenced to the NIST standard lamp for example) should be mounted at a port on the outer wall of integrating sphere, the spectra with only calibration lamp and only device holder is then measured. The ratio between the two measured intensities gives the Auxiliary spectra, equation 7.

$$R(\lambda) = \frac{P_{cal}(\lambda)}{I_{cal}(\lambda)} \quad (6)$$

$$A(\lambda) = \frac{I_{aux,cal}(\lambda)}{I_{aux,dev}(\lambda)} \quad (7)$$

The power spectrum, $P_{device}(\lambda)$ of the device is then given by the product of the response of the system to the auxiliary correction and the current of the device,

equation 8. This allows for the calculation of the power efficiency, η_p by integrating the power spectrum over wavelength divided by the electrical power, equation 9.

$$P_{device}(\lambda) = A(\lambda) \cdot R(\lambda) \cdot I_{device}(\lambda) \quad (8)$$

$$\eta_p = \frac{\int_{\lambda} P_{device}(\lambda) d\lambda}{VI} \quad (9)$$

Finally, for the E.Q.E., it is necessary to convert the power at each wavelength to the number of photons emitted per second, followed by integration over wavelength and the ratio by the number of electrons flowing into the device per second, equations 10 and 11.

$$\eta_B = \int_{\lambda} \frac{P(\lambda)c}{\hbar\lambda} d\lambda \quad (10)$$

$$\eta_{ext} = \frac{\eta_B e}{I} \quad (11)$$

With such a full correction in place, the basic characterization of OLED devices can be made, and **Figure 9** gives an example of this characterization, from the same device shown in **Figure 8**. Lastly, it is very important to note that only the light emitted in the forward direction of the OLED should be measured to obtain the true EQE. This requires that the edges of the device be covered to prevent wave guided light escaping from the edges of the glass substrate entering into the sphere. This light which in real application is unusable can greatly affect the measurement, artificially (and incorrectly) increasing EQE. As a reality check, IQE cannot exceed 100%. In a) the turn-on voltage of this device can be extrapolated (3.5 V), being the voltage at which the device starts operating. Also, the maximum luminance can be seen (10.000 cd/m²), which can be used to compare with other light sources and research-based devices. In b) the evolution of the E.Q.E. is seen, the maximum efficiency given at the specific luminance (i=13.6 % at 200 cd/m²). Also in b) the efficiency roll-off with the critical luminance value L_{90%} [20] defined as the luminance at which the efficiency drops to 90% of its maximum value can be calculated (ii=400 cd/m²). This decrease is a result of an overlapping of different excited state annihilation processes, such as polaron–exciton and exciton–exciton annihilation, field-induced quenching, charge carrier imbalance, Joule heating and degradation,

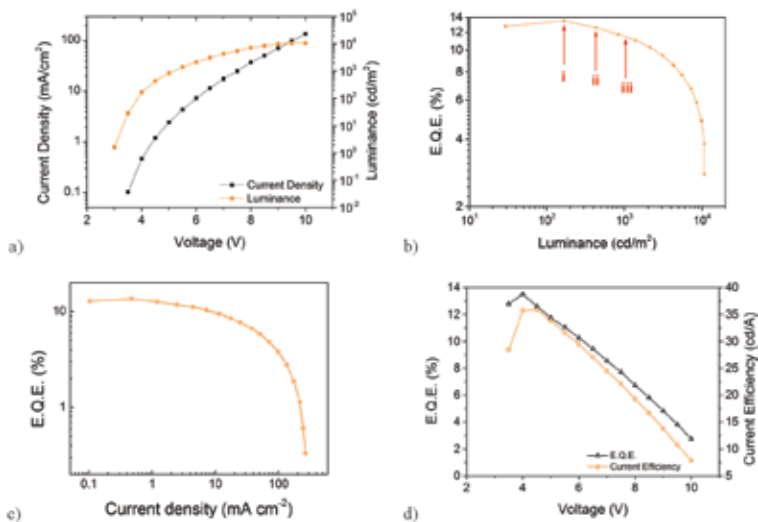


FIGURE 9

OLED electrical characterization for the TADF-based green OLED of figure 8. a) Current Density-Voltage-Luminance, b) External Quantum Efficiency - Luminance, c) External Quantum Efficiency - Current Density and d) External Quantum Efficiency - Current Density - Voltage. All values are were taken from the dependance of voltage.

all reviewed elsewhere [20]. Finally, the values at the practical luminance of 1000 cd/m² (iii) are also taken and used for comparison aspects. Up to a certain voltage, device degradation starts to become visible, resulting in a decrease of luminance and efficiency. This becomes relevant at luminance values of 1000 cd/m². Both c) and d) show how the device operates at different current densities, which can give information on power consumptions and stability with potential.

6. CONCLUSIONS

Different aspects regarding the physical operation and characterization of Organic Light Emitting Diodes (OLEDs) were reviewed. Depending on the application in mind, either the colour of the device or its efficiency (or even both) must be optimized and so, different characterization aspects must be chosen accordingly. Different research groups tend to focus on different aspects of the physical internal and external characteristics of these devices such as synthesizing molecules capable of high internal efficiency, or optimizing the light out-coupling or even the production White OLEDs with high colour quality. The care required in making device measurements in an integrating sphere cannot be stressed enough, it is very easy to introduce large

errors by cutting corners! The authors hope this review shed light on different electrical and optical considerations while showing how to prepare a device characterization lab.

REFERENCES

- [1] C. W. Tang and S. A. Vanslyke, "Organic electroluminescent diodes," *Appl. Phys. Lett.*, vol. 51, no. 12, pp. 913–915, 1987.
- [2] J. François Tremblay, "The rise of OLED displays," *Chemical & Engineering News*, 2016. [Online]. Available: <http://cen.acs.org/articles/94/i28/rise-OLED-displays.html>. [Accessed: 04-Oct-2016].
- [3] R. Mertens, "LGD's Gen-5 OLED lighting fab is progressing according to plan, will enter production in 2017," *OLED-info*, 2016. [Online]. Available: <http://www.oled-info.com/lgds-gen-5-oled-lighting-fab-progressing-according-to-plan-will-enter-production-2017>. [Accessed: 04-Oct-2016].
- [4] J. B. B. Richter, U; Vogel, R. Herold; K. Fehse; S. Brenner; L. Kroker, "Bidirectional OLED Microdisplay: Combining Display and Image Sensor Functionality into a Monolithic CMOS chip," in *IEEE*, 2011, p. 314.
- [5] S. Reineke, M. Thomschke, B. Lüssem, and K. Leo, "White organic light-emitting diodes: Status and perspective," *Rev. Mod. Phys.*, vol. 85, no. 3, pp. 1245–1293, 2013.
- [6] L. S. Cui, J. U. Kim, H. Nomura, H. Nakanotani, and C. Adachi, "Benzimidazobenzothiazole-based Bipolar Hosts to Harvest Nearly All of the Excitons from Blue Delayed Fluorescence and Phosphorescent Organic Light-Emitting Diodes," *Angew. Chemie - Int. Ed.*, pp. 1–6, 2016.
- [7] R. S. Nobuyasu, Z. Ren, G. C. Griffiths, A. S. Batsanov, P. Data, S. Yan, A. P. Monkman, M. R. Bryce, and F. B. Dias, "Rational Design of TADF Polymers Using a Donor-Acceptor Monomer with Enhanced TADF Efficiency Induced by the Energy Alignment of Charge Transfer and Local Triplet Excited States," *Adv. Opt. Mater.*, no. August 2016, 2016.
- [8] N. Thejo Kalyani and S. J. Dhoble, "Organic light emitting diodes: Energy saving lighting technology - A review," *Renew. Sustain. Energy Rev.*, vol. 16, no. 5, pp. 2696–2723, 2012.
- [9] P. R. Boyce, "Fundamentals: Photometric Quantities," in *Human factors in lighting - 3rd Edition*, 3rd ed., CRC Press, 2014, pp. 6–10.
- [10] A. P. Monkman, C. Rothe, and S. M. King, "Singlet generation yields in organic light-emitting diodes," *Proc. IEEE*, vol. 97, no. 9, pp. 1597–1605, 2009.
- [11] J.-H. Jou, S. Kumar, A. Agrawal, T.-H. Li, and S. Sahoo, "Approaches for fabricating high efficiency organic light emitting diodes," *J. Mater. Chem. C*, vol. 3, no. 3, pp. 2974–3002, 2015.
- [12] F. B. Dias, K. N. Bourdakos, V. Jankus, K. C. Moss, K. T. Kamtekar, V. Bhalla, J. Santos, M. R. Bryce, and A. P. Monkman, "Triplet harvesting with 100% efficiency by way of thermally activated delayed fluorescence in charge transfer OLED emitters," *Adv. Mater.*, vol. 25, no. 27, pp. 3707–3714, 2013.
- [13] T.-A. Lin, T. Chatterjee, W.-L. Tsai, W.-K. Lee, M.-J. Wu, M. Jiao, K.-C. Pan, C.-L. Yi, C.-L. Chung, K.-T. Wong, and C.-C. Wu, "Sky-Blue Organic Light Emitting Diode with 37% External Quantum Efficiency Using Thermally Activated Delayed Fluorescence from Spiroacridine-Triazine Hybrid," *Adv. Mater.*, 2016.
- [14] W. Youn, J. Lee, M. Xu, R. Singh, and F. So, "Corrugated Sapphire Substrates for Organic Light-Emitting Diode Light Extraction," *ACS Appl. Mater. Interfaces*, vol. 7, no. 17, pp. 8974–8978, 2015.
- [15] "CIE - Commission Internationale d'Eclairage." [Online]. Available: http://div2.cie.co.at/?i_ca_id=985.
- [16] V. K. Khanna, *Fundamentals of Solid-State Lighting*, no. 518. 2014.

- [17] R. W. G. Hunt and M. Pointer, *Measuring Colour*. 2011.
- [18] D. Pereira, A. Pinto, A. California, J. Gomes, and L. Pereira, "Control of a White Organic Light Emitting Diode's emission parameters using a single doped RGB active layer," *Mater. Sci. Eng. B*, vol. 211, no. September, pp. 156–165, 2016.
- [19] P. L. dos Santos, J. S. Ward, P. Data, A. Batsanov, M. R. Bryce, F. Dias, and A. P. Monkman, "Engineering the singlet-triplet energy splitting in a TADF molecule," *J. Mater. Chem. C*, vol. 4, no. ii, pp. 3815–3824, 2016.
- [20] C. Murawski, K. Leo, and M. C. Gather, "Efficiency roll-off in organic light-emitting diodes," *Adv. Mater.*, vol. 25, no. 47, pp. 6801–6827, 2013.